

Multi-strange baryon production in Au+Au collisions near threshold

Gebhard Zeeb, Manuel Reiter, and Marcus Bleicher

*Institut für Theoretische Physik,
J. W. Goethe-Universität,
Robert-Mayer-Str. 8-10, 60054 Frankfurt am Main, Germany*

The centrality dependence of Ξ^- and Λ production in Au+Au interactions at $E_{\text{lab}} = 6 \text{ AGeV}$ is studied within a microscopic transport approach. In line with recent data, a slight enhancement of the $\Xi^-/(\Lambda + \Sigma^0)$ ratio toward central collisions is found. It is demonstrated that the observed production of multiple strange baryons can be traced back to multi-step meson-baryon interactions in the late stages of the collisions. Therefore, the present analysis supports an interpretation of the observed Ξ abundance in terms of hadronic re-scattering.

The major goal of the various heavy ion programs is the search for a transient state of deconfined matter, dubbed the quark-gluon-plasma (QGP): A phase transition to this new state of matter is predicted by lattice QCD when a sufficiently high energy density ($\epsilon \approx 1 \text{ GeV/fm}^3$) is reached [1].

Strange particle yields and spectra are key probes to study excited nuclear matter and to detect the transition of (confined) hadronic matter to quark-gluon-matter, i.e. QGP [1,2]. The relative enhancement of strange and multi-strange hadrons, as well as hadron ratios in central heavy ion collisions with respect to peripheral or proton induced interactions have been suggested as a signature for the transient existence of a QGP phase [2].

A wealth of systematic information has been gathered to study the energy dependence of observables from $\sqrt{s} \approx 2 \text{ AGeV}$ to $\sqrt{s} = 200 \text{ AGeV}$. For the first time also information on the Ξ near threshold is available [3].

For our investigation, the Ultra-relativistic Quantum Molecular Dynamics model (UrQMD 1.2) [4] is applied to heavy ion reactions from $E_{\text{lab}} = 2 \text{ AGeV}$ to 10 AGeV . This microscopic transport approach is based on the covariant propagation of constituent quarks and diquarks accompanied by mesonic and baryonic degrees of freedom. It describes multiple interactions of ingoing and newly produced particles, the excitation and fragmentation of color strings and the formation and decay of hadronic resonances. Toward higher energies, the treatment of sub-hadronic degrees of freedom is of major importance. In the present model, these degrees of freedom enter via the introduction of a formation time for hadrons produced in the fragmentation of strings [5–7]. The leading hadrons of the fragmenting strings contain the valence-quarks of the original excited hadron. In UrQMD they are allowed to interact even during their formation time, with a reduced cross section defined by the additive quark model, thus accounting for the origi-

nal valence quarks contained in that hadron [4]. A phase transition to a quark-gluon state is not incorporated explicitly into the model dynamics. However, a detailed analysis of the model in thermal equilibrium yields an effective equation of state of Hagedorn type [8,9].

Note that the present calculations have been performed without potential interactions. Thus, no in-medium modifications of hadron masses and widths are taken into account.

Figure 1 (top and middle panel) shows the centrality dependence of the Ξ^- and Λ yields in Au+Au interactions at $E_{\text{lab}} = 6 \text{ AGeV}$.

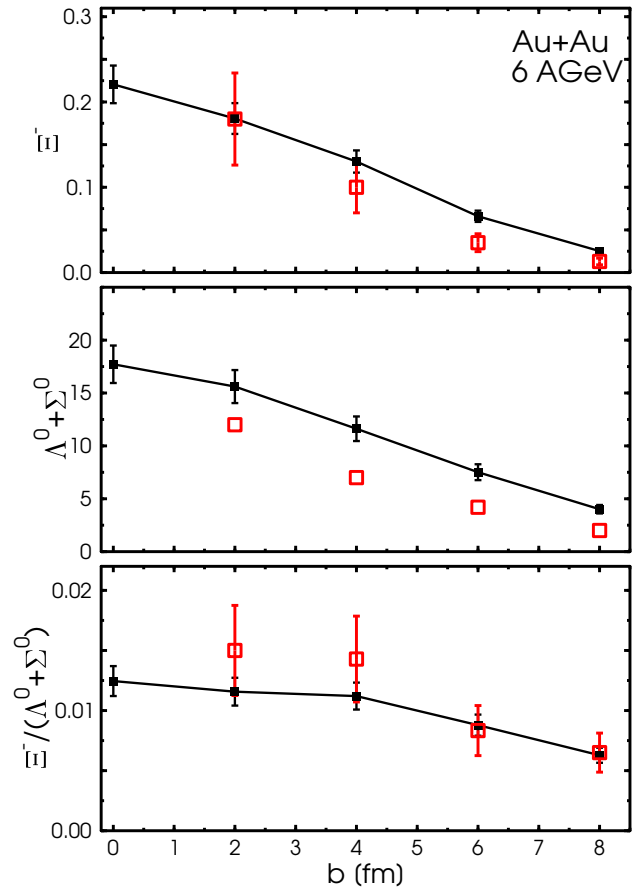


FIG. 1. Centrality dependence of the ratio $\Xi^-/(\Lambda + \Sigma^0)$ (bottom) and the Λ (middle) and Ξ^- (top) yields in Au+Au interactions at $E_{\text{lab}} = 6 \text{ AGeV}$. Small symbols denote the calculations, while large symbols show the data from [3].

One clearly observes a strong increase of the (multi-)strange baryon yields toward head-on collisions. However, at all energies from 2-10 AGeV, the Cascade yield increases stronger than the single strange hyperon abundance toward central collisions. This leads to a moderate centrality dependence of the Ξ^-/Λ ratio as shown in Fig. 1 (bottom) explicitly for a beam energy of 6 AGeV. The centrality dependent yields (small symbols show the calculations, while large symbols denote the experimental data taken from [3]) as well as the ratios show good agreement with the recently measured data of the E895 collaboration.

Let us now focus on the dynamics of the Cascade production. In the present approach the increase in strangeness production towards central interactions is due to multi-step processes. I.e., Primary interactions lead to the production of

1. heavy mesons and baryons
2. as well as Λ and Σ hyperons and anti-Kaons.

In subsequent interactions, the collisions of those excited meson/baryon resonances can more easily result in the production of a Cascade, due to their increased center of mass energy. In Ref. [10], a similar mechanism has been advocated to understand the production of anti-baryons around threshold energies. In addition, meson interactions with previously formed hyperons have also an increased chance for Ξ production, because only one additional unit of strangeness has to be produced. Finally strangeness exchange reactions, e.g. $\bar{K} + \Lambda \rightarrow \Xi + \pi$, can have a major contribution to the finally observed Cascade abundance.

Three processes and classes of channels for Ξ production can be identified:

- Reactions between baryons (BB), i.e. $BB \rightarrow \Xi + x$.
- Meson-baryon reactions (MB), i.e. $MB \rightarrow \Xi + x$.
- Decays of baryon resonances, i.e. $\Xi^* \rightarrow \Xi + x$.

Note that Ξ includes also $\Xi^*(1530)$, since the $\Xi^*(1530)$ decays to 100% into Ξ . Throughout this paper, Ξ^* denotes all Cascade resonances, except the $\Xi^*(1530)$.

In the following, we will investigate these production channels in more detail. First, it is demonstrated that Cascades are formed in the late stages of central heavy ion interactions at AGS energies. Figure 2 shows the Ξ production rate as a function of time in central Au+Au reactions at 6 A GeV divided into the contribution from baryon-baryon (BB), meson-baryon (MB) interactions and decay channels. A clear separation in time shows up when comparing the different channels: The baryon-baryon channel (dashed line) has its production peak at maximum overlap time of the penetrating nuclei at $t_{\max, BB} \approx 6$ fm/c. Then, Ξ production from the cooking meson-baryon "soup" sets in (full line). Here the maximum is at times around $t_{\max, MB} \approx 8$ fm/c. Up

to 13 fm/c the production rate in the meson-baryon channel is higher than the maximum production rate in baryon-baryon collisions. This clearly indicates the importance of secondary interaction processes for multi-strange baryon production in this energy range. The late contribution - from the decay of high mass Ξ resonances (dotted line) - is tiny. The production of Cascades stretches over nearly 10 fm/c. Thus, multi-strange baryon production relies on long living hadronic stages, which might allow for chemical equilibration even in this exotic channel.

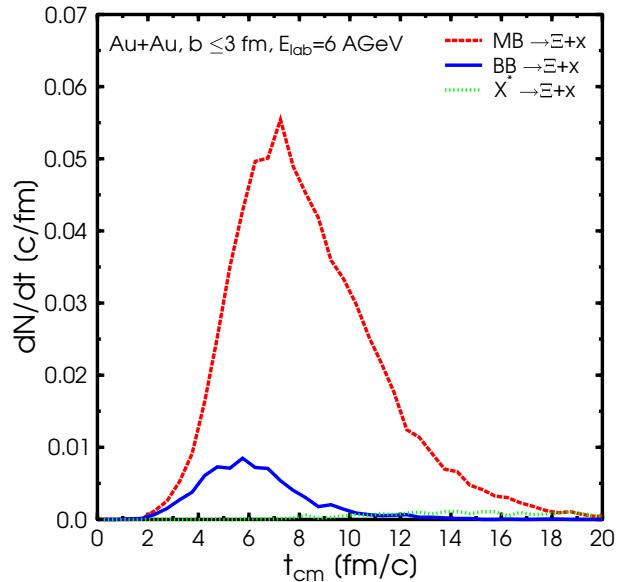


FIG. 2. Differential production times of Ξ particles in central Au+Au reactions at $E_{\text{lab}} = 6$ AGeV broken down to the different channels.

It is noteworthy that also other scenarios for an enhanced production of multi-strange baryons are possible. E.g. a mass reduction of the Ξ might yield considerably larger contributions from baryon-baryon scatterings, since at the time of complete overlap baryon densities are highest. It is hard to distinguish between our scenario (without in-medium modifications) and a calculation with in-medium effects included solely on the basis of total multiplicities. A detailed study of the in-plane and out-of-plane flow might allow deeper insight into the underlying production mechanisms.

Figure 3 gives the production channel decomposition of Cascades in central Au+Au reactions at $E_{\text{lab}} = 6$ A GeV. The leading production channel is from meson-baryon reactions, followed by the baryon-baryon channel. The decay of higher mass resonances into a Ξ is only of minor importance. Meson-meson interactions do not contribute to the Ξ production due to their small number and low center of mass energies.

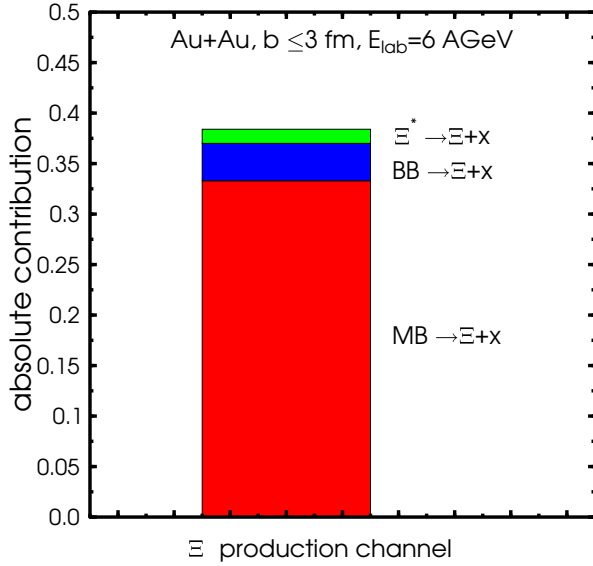


FIG. 3. Channel decomposition of reactions leading to the production of Ξ particles in central Au+Au reactions at $E_{\text{lab}} = 6$ AGeV.

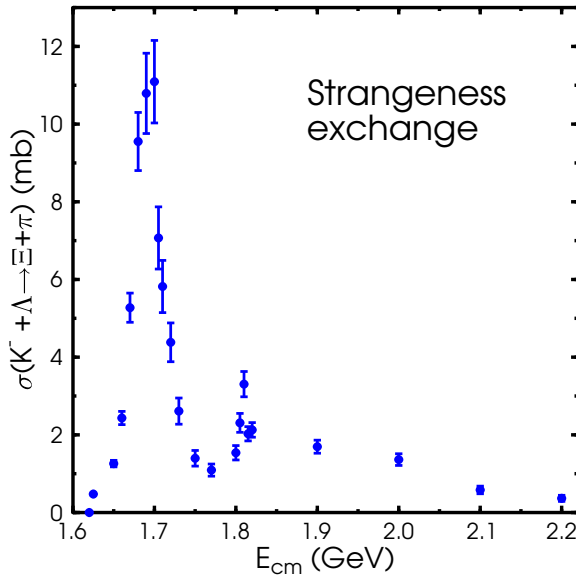


FIG. 4. Exclusive cross section for the strangeness exchange in $K^- + \Lambda \rightarrow \Xi + \pi$ as a function of the center of mass energy.

Let us have a deeper look into the leading production channels. It has been suggested in [11] (within the ART transport model) that strangeness exchange reactions, e.g. $\bar{K}(\Lambda, \Sigma) \leftrightarrow \Xi\pi$, are the most prominent Ξ creation

channels. However, the present study indicates that also OZI forbidden channels yield a huge contribution to the Cascade production cross section. To make the present work comparable to the analysis by [11], Fig. 4 gives the cross section for the reaction $K^- + \Lambda \rightarrow \Xi + \pi$ as employed in the present calculation. However, note that the presented strangeness exchange channel is implicitly given by the baryon resonances and string break-up mechanism included in the model. Possible reasons for the differences between the models are (I) the omission of high mass meson and baryon resonances in the ART model and (II) a more than twice as large $\bar{K} + \Lambda \rightarrow \Xi + \pi$ cross section in the calculation by [11] compared to our cross section.

The contribution of the baryon-baryon collisions to the Ξ production is dominated by $N + \Lambda$ (42%) and $(\Delta, N^*) + \Lambda$ (48%), here Δ, N^* denotes all Delta and N^* resonances. The missing 10% of BB interactions are the contributions of all remaining types of BB interactions. In the meson-baryon sector, three distinct groups of reactions dominate the Ξ production at the investigated energy as shown in table I. The channels η , η' , $a_0(980)$, $a_1(1260)$, $a_2(1320)$ and $b_1(1235)$ interacting with a baryon, do contribute with 16%.

Channel	Percentage
$(\bar{K}, \bar{K}^*(892)) + B$	33 %
$\pi + B$	24 %
$(\rho, \omega) + B$	22 %
$(\eta, \dots, b_1(1235)) + B$	16 %
other MB reactions	5 %
Total	100 %

TABLE I. Decomposition of the dominant meson induced channels to the Ξ production.

Reaction	rel.	abs.
$(\bar{K}, \bar{K}^*(892)) + N$	11 %	3.7 %
$(\bar{K}, \bar{K}^*(892)) + N^*$	21 %	6.9 %
$(\bar{K}, \bar{K}^*(892)) + \Delta$	34 %	11.2 %
$(\bar{K}, \bar{K}^*(892)) + \Lambda, \Sigma$	34 %	11.2 %
Total	100 %	33.0 %
$\pi + (\Lambda, \Sigma)$	91 %	21.8 %
$\pi + \text{other baryon}$	9 %	2.2 %
Total	100 %	24.0 %
$(\rho, \omega) + (\Lambda, \Sigma)$	98 %	21.6 %
$(\rho, \omega) + \text{other baryon}$	2 %	0.4 %
Total	100 %	22.0 %
$(\eta, \dots, b_1(1235)) + N$	14 %	2.2 %
$(\eta, \dots, b_1(1235)) + \Delta$	7 %	1.1 %
$(\eta, \dots, b_1(1235)) + \Lambda, \Sigma$	76 %	12.2 %
$(\eta, \dots, b_1(1235)) + \text{other baryon}$	3 %	0.5 %
Total	100 %	16 %

TABLE II. Classification of the baryon types in meson induced reactions leading to the production of a Cascade.

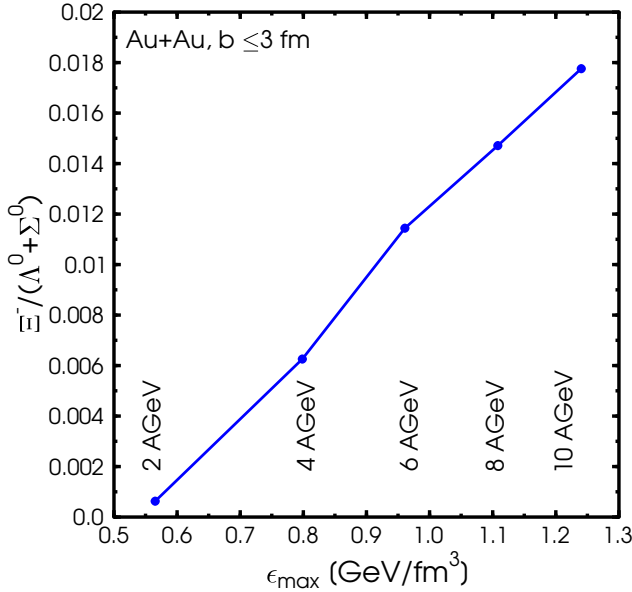


FIG. 5. The ratio $\Xi^-/(\Lambda + \Sigma^0)$ in central Au+Au reactions as a function of the maximal energy density achieved at incident energies from 2 AGeV to 10 AGeV.

The Kaon channel is dominated by the \bar{K} with 59% of all \bar{K} induced MB reactions and $\bar{K}^*(892)$ (27%). The six high mass anti-Kaon resonances do each contribute 0.6% - 4%. The different meson induced channels are given explicitly in table II.

From the detailed analysis presented, it is evident that Ξ production is mainly driven by meson-baryon interactions including a Λ or Σ . In fact, 70% of all meson-baryon reactions resulting in the production of a Cascade include a hyperon. However, the present analysis indicates that only 11% of the MB interactions leading to Ξ production proceed via the strangeness exchange reaction anti-Kaon + hyperon, in strong contrast to Ref. [11].

Why is the energy range of $E_{\text{lab}} = 2$ to 10 AGeV so interesting and important? This becomes obvious by studying the maximal achieved energy density in this energy region. Figure 5 shows the ratio Ξ^-/Λ in central Au+Au reactions as a function of maximal energy density reached in collision at different incident energies. At a beam energy of 6 AGeV, the model predicts to cross the critical energy density of 1 GeV/fm³. The present calculation predicts a linear dependence of $\Xi^-/(\Lambda + \Sigma^0)$ on the energy density. Therefore, it is important to study deviations from this scaling to identify a possible onset of additional strangeness enhancement from non-hadronic sources.

Finally, we compare the model calculations to $\Xi^-/(\Lambda + \Sigma^0)$ ratios obtained at higher energies. Figure 6 shows the default UrQMD simulation (open circles),

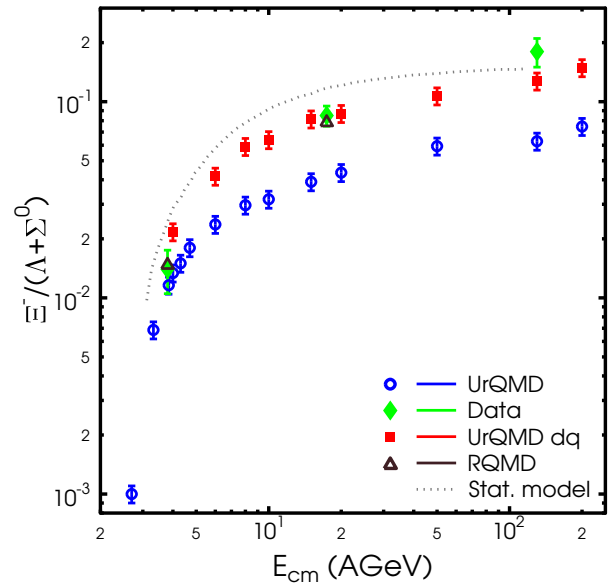


FIG. 6. Energy dependence of the $\Xi^-/(\Lambda + \Sigma^0)$ ratio in Au+Au/Pb+Pb collisions. The UrQMD calculations ($b = 2$ fm) are shown by circles. UrQMD with the inclusion of di-quark clusters is depicted by the squares. The dotted line indicates the results of a statistical model [12], while the triangles show RQMD results. The data (diamonds) are taken from [13].

a calculation with strange di-quark clustering¹ enabled (open squares) in comparison to a statistical model prediction [12] (line) and the available data [13] (full diamonds). In the AGS energy range, the hadronic dynamics are clearly able to describe the data. Also, the microscopic simulation and the statistical model agree well at low energies. With increasing center of mass energy, however, the default simulation clearly underpredicts the yield of double strange baryons, resulting in an underprediction of the $\Xi^-/(\Lambda + \Sigma^0)$ ratio at SPS and RHIC. It is possible to obtain a reasonable description of the Ξ^- abundances, if additional mechanisms like di-quark clustering (employed in this investigation) or string fusion (see Ref. [14–16], RQMD results are depicted by triangles).

In summary, we have used a relativistic hadronic transport model to investigate the production of multi-strange baryons in high density nuclear matter. Comparing the calculation with the recent data by the E895 collaboration indicates a good description of the data within the present hadronic model. In fact the nice agreement between experimentally observed yield and the present

¹This option is available with the input parameter cto 37 set to 1.

calculation in the AGS energy range is in stark contrast to the results obtained at SPS energies. There hadronic transport models without non-standard modifications clearly fail to describe the measured Ξ yields. We find that meson-baryon reactions not only between anti-Kaons and hyperons but also with non-strange particles lead to a substantial production of Ξ^- in Au+Au collisions around 6 A GeV. Within the present model, the $\Xi/(\Lambda + \Sigma^0)$ ratio is proportional to the energy density.

ACKNOWLEDGEMENTS

The authors acknowledge stimulating discussions with Dr. Helmut Oeschler at Darmstadt University of Technology. This work used computational resources provided by the Centre Calculé at Lyon, France, and the Center for Scientific Computing (CSC) at Frankfurt, Germany. This work was supported by GSI, BMBF, DFG.

K. Redlich, Nucl. Phys. A **697** (2002) 902 [arXiv:hep-ph/0106066].

- [13] SPS energy: S. V. Afanasiev et al. (NA49 Collaboration), Phys. Lett. B538 (2002) 275; A. Mischke et al. (NA49 Collaboration), J. Phys. G28 (2002) 1761.
- RHIC energy: J. Castillo et al. (STAR Collaboration), Proceedings of the Quark Matter 2002. Note that the RHIC data refers to midrapidity and not 4π .
- [14] H. Sorge, Phys. Rev. C **52** (1995) 3291 [arXiv:nucl-th/9509007].
- [15] H. Sorge, Nucl. Phys. A **630** (1998) 522 [arXiv:nucl-th/9707021].
- [16] S. Soff, S. A. Bass, M. Bleicher, L. Bravina, E. Zabrodin, H. Stocker and W. Greiner, Phys. Lett. B **471** (1999) 89 [arXiv:nucl-th/9907026].

- [1] S.A. Bass, M. Gyulassy, H. Stöcker and W. Greiner, J. Phys. **G25**, R1 (1999);
R. Stock, Phys. Lett. **B456**, (1999) 277
- [2] J. Rafelski and B. Müller, Phys. Rev. Lett. **48**, 1066 (1982); J. Rafelski, Phys. Rep. **88**, 331 (1982);
P. Koch, B. Müller and J. Rafelski, Phys. Rep. **142**, 167 (1986).
- [3] P. Chung *et al.* (E895 collaboration), Phys. Rev. Lett. **91** (2003) 202301 [arXiv:nucl-ex/0302021].
- [4] M. Bleicher, E. Zabrodin, C. Spieles, S.A. Bass, C. Ernst, S. Soff, L. Bravina, M. Belkacem, H. Weber, H. Stöcker, W. Greiner, J. Phys. G **25** (1999) 1859 [arXiv:hep-ph/9909407];
S.A. Bass, M. Belkacem, M. Bleicher, M. Brandstetter, L. Bravina, C. Ernst, L. Gerland, M. Hofmann, S. Hofmann, J. Konopka, G. Mao, L. Neise, S. Soff, C. Spieles, H. Weber, L.A. Winckelmann, H. Stöcker, W. Greiner, C. Hartnack, J. Aichelin, N. Amelin, Prog. Part. Nucl. Phys. **41** (1998) 225 [arXiv:nucl-th/9803035];
A Woods-Saxon initialization for each nucleus is used (i.e. CTOption 24 = 1).
- [5] B. Andersson, G. Gustavson, B. Nilsson-Almquist, Nucl. Phys. **B281**, 289 (1987).
- [6] B. Andersson *et al.*, Comp. Phys. Comm. **43**, 387 (1987).
- [7] T. Sjöstrand, Comp. Phys. Comm. **82**, 74 (1994).
- [8] M. Belkacem *et al.*, Phys. Rev. C **58** (1998) 1727 [arXiv:nucl-th/9804058].
- [9] L.V. Bravina *et al.*, Phys. Rev. C **60** (1999) 024904 [arXiv:hep-ph/9906548].
- [10] C. Spieles, A. Jahns, H. Sorge, H. Stocker and W. Greiner, Mod. Phys. Lett. A **8** (1993) 2547.
- [11] S. Pal, C. M. Ko, J. M. Alexander, P. Chung and R. A. Lacey, arXiv:nucl-th/0211020.
- [12] P. Braun-Munzinger, J. Cleymans, H. Oeschler and